

ChemComm

Accepted Manuscript



This is an *Accepted Manuscript*, which has been through the Royal Society of Chemistry peer review process and has been accepted for publication.

Accepted Manuscripts are published online shortly after acceptance, before technical editing, formatting and proof reading. Using this free service, authors can make their results available to the community, in citable form, before we publish the edited article. We will replace this *Accepted Manuscript* with the edited and formatted *Advance Article* as soon as it is available.

You can find more information about *Accepted Manuscripts* in the [Information for Authors](#).

Please note that technical editing may introduce minor changes to the text and/or graphics, which may alter content. The journal's standard [Terms & Conditions](#) and the [Ethical guidelines](#) still apply. In no event shall the Royal Society of Chemistry be held responsible for any errors or omissions in this *Accepted Manuscript* or any consequences arising from the use of any information it contains.

Dual Selective Iron Chelating Probes with a Potential to Monitor Mitochondrial Labile Iron Pools†

Vincenzo Abbate ‡^a, Olivier Reelfs ‡^b, Xiaole Kong ^a, Charareh Pourzand,^b and Robert C. Hider^{a*}

Received (in XXX, XXX) Xth XXXXXXXXX 200X, Accepted Xth XXXXXXXXX 200X

First published on the web Xth XXXXXXXXX 200X

DOI: 10.1039/b000000x

Mitochondria-targeted peptides incorporating dual fluorescent and selective iron chelators have been designed as novel biosensors for the mitochondrial labile iron pool. The probes were demonstrated to specifically co-localize with mitochondria and their fluorescence emission was found to be sensitive to the presence of iron.

Mitochondria are the primary sources of energy for cells in the form of ATP. Given this fundamental activity, defects in mitochondrial function have severe physiological effects¹. Indeed, abnormalities of mitochondrial DNA and oxidative phosphorylation have been identified in several neurodegenerative diseases. It is thus extremely important to be able to accurately monitor mitochondrial activity in order to identify potential malfunctions of this fundamental organelle.

Despite iron homeostasis being tightly controlled, under conditions of oxidative stress and in certain pathologies the normal iron binding capacity of cells may be exceeded, resulting in the appearance of the redox-active chelatable Labile Iron Pool (LIP)². This in turn leads to an increase in the production of free radicals due to iron-catalyzed Reactive Oxygen Species (ROS) transformation via the Fenton reaction³, with detrimental consequences for the cell. There is increasing experimental evidence demonstrating that iron overload and oxidative stress play a key role in cell damage caused by solar UVA irradiation^{2,4} and in neurodegenerative disorders, including Alzheimer's disease⁵, Parkinson's disease⁶ and Friedreich's ataxia⁷. In particular, mitochondria have been identified as critical organelles hosting LIP-induced chains of oxidative events. This clearly highlights the need for the development of reliable probes for mitochondrial LIP monitoring.

Much effort has been devoted to the design and development of chemical tools which are capable of specifically targeting mitochondria. Lipophilic cations comprising of a triphenyl phosphine (TPP) head linked to a cargo represent an established class of such molecules⁸. More recently, a novel class of small cationic aromatic peptides has been described, which possess the ability to both efficiently penetrate cell membranes in an energy-independent, non-saturable manner and to rapidly accumulate in the mitochondria⁹. Such a system has been exploited for the development of antioxidants¹⁰ and antimicrobials¹¹.

In order to better understand the role of LIP in mitochondrial oxidative disorders, we recently reported a series of bidentate, selective iron(III)-chelators conjugated to fluorescent mitochondria-targeting peptides (Fig. 1)¹². Such probes were

demonstrated to possess cell-penetrating capability and to preferentially accumulate in mitochondria. Furthermore, the targeted iron chelators were found to be sensitive to the presence of iron via an energy-transfer mechanism causing progressive fluorophore quenching at increasing iron(III) concentrations. However, the chemical assembly of these compounds requires challenging conjugation of an iron chelator and a fluorophore in two different positions of a simple tetrapeptide, inevitably perturbing the native peptide structure.

In this communication, we report the design and biological evaluation of a second generation of cell-penetrating, dual fluorescent and selective iron chelators targeted to the mitochondria (Fig. 2). Here, both fluorophore and metal chelating centres are located on the same structural moiety, allowing more efficient chemical synthesis, and leading possibly to more organelle-selective intracellular trafficking of the chelator. Furthermore, this "intrinsically fluorescent" iron chelating compound class possesses improved physico-chemical properties, including quantum yield and molar extinction coefficient¹³, when compared to the dansyl moiety¹⁴, rendering them more attractive LIP-sensing candidates. The structures of the newly designed compounds are depicted in Figure 2. We have adopted the bidentate 2-hydroxypyridin-4-one as scavenger of iron. This chelator has high affinity for iron(III), but will also bind iron(II) subsequently autoxidising the metal to iron(III). This latter property leads only to the partial chelation of iron(II) at concentrations less than 10 μ M and therefore the molecules are able to sense the iron(II) levels. These chelating units are highly selective for iron under biological conditions¹³.

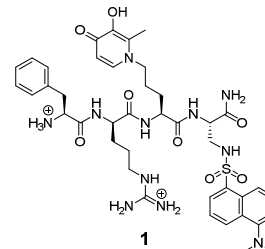


Fig. 1 A fluorescent mitochondria-targeted peptide incorporating an iron chelator¹².

Compound **1** was designed and prepared in isomerically pure form (see ESI) and protected with a benzyl group ready for on-resin conjugation to either orthogonally deprotected lysine (**3**, **6** or **7**) or diaminopropionic acid (DAP) (**4-5**) or

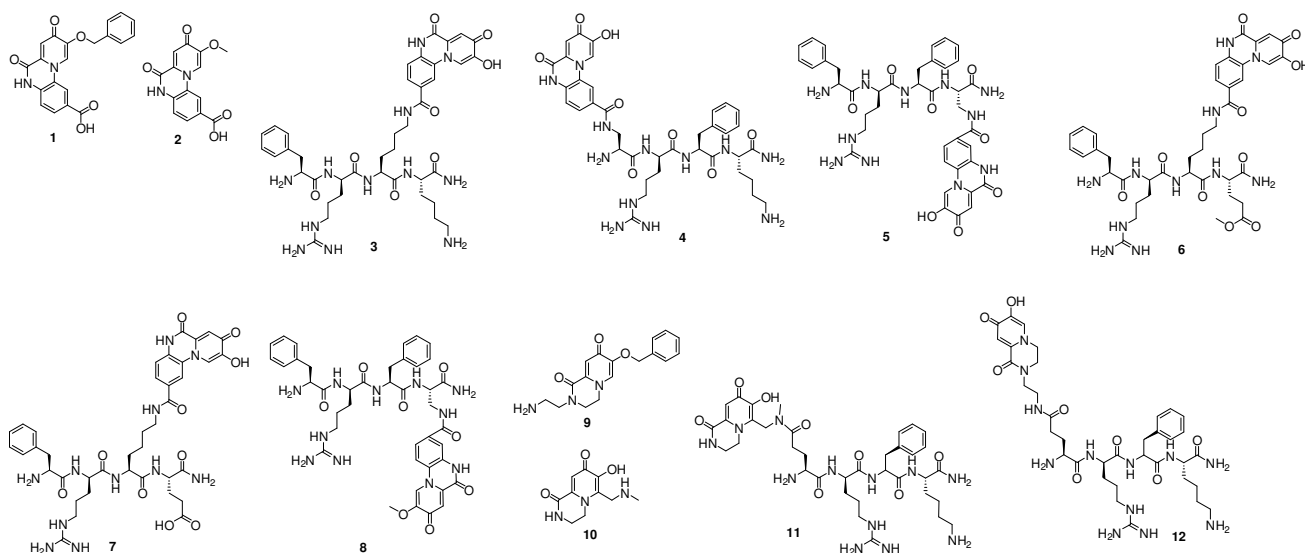


Fig. 2 Structures of dual fluorescent iron chelators and iron chelating peptides.

5 corresponding peptide chains.

A panel of probes was thus prepared where the dual fluorescent iron chelator replaced a Phe-residue in the central part of the tetrapeptide sequence (3, 6-7), at the N-terminus (4) or replaced the C-terminal lysine (5). In order to investigate the role of the peptide net charge on the cell-penetration and the intracellular trafficking, compound 7 was prepared where the C-terminal lysine was substituted by a negatively-charged moiety. Compound 8 represents a structural analogue of 5 where a protected iron chelating moiety, namely compound 2, was incorporated in the structure; here the hydroxyl group on the pyridinone ring is methylated and consequently lacks the ability to coordinate iron(III). To further expand the chemical versatility of the solid-phase approach, compounds 11 and 12 were designed where by an orthogonally protected glutamic acid residue was activated on the solid support for the selective conjugation of either primary- (compound 9) or secondary- (compound 10) amine containing 3-hydroxypyridinones (HPOs). This led to a subset of more polar peptide-chelators, given that compounds 9 and 10 contain a bicyclic structure, as compared to the tricyclic compounds 1-2. Moreover, compound 10 does not bear a protecting group on the 3-hydroxyl position in the HPO ring, demonstrating that the conjugation chemistry employed for peptide 12 synthesis is compatible with an unprotected iron chelator.

Cleavage of the peptides from the resin followed by the BCl_3 -mediated deprotection of the benzyl group afforded crude products which were purified via semi-preparative HPLC. Purity of the final compounds was assessed by analytical RP-HPLC and HRES-MS (ESI).

To ascertain that such peptides possessed high affinity for iron, spectrophotometric titrations were conducted (ESI, Fig. S3) and the pFe^{3+} value for peptide 4 was determined to be 21.5. A value greater than 20 is required for effective iron

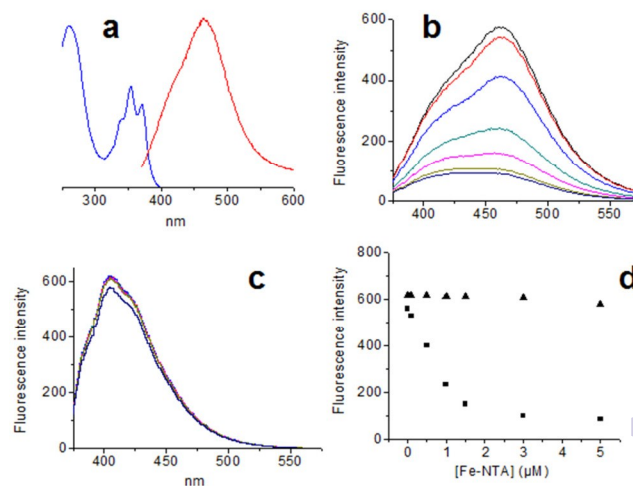


Fig. 3 (a) UV-vis (blue line) and fluorescent (red line) spectra of compound 3; fluorescence emission spectra of 3 (panel b) and 8 (panel c) in the presence of increasing amount of iron(III) ($\lambda_{\text{ex}} = 350 \text{ nm}$); (d) fluorescence quenching of 3 (squares) and 8 (triangles) in the presence of iron(III).

scavenging in biological matrices¹⁵. The spectroscopic properties of the ligands and peptides were studied via UV-vis and fluorescence spectroscopies (Fig. 3a). The peptide-chelator conjugates possess at least three excitation maxima in the region of 260 nm, 350 nm and 370 nm. The emission maxima of the peptides ranged between 410-425 nm.

To determine whether the mitochondria-targeted chelators were sensitive to the presence of iron(III), buffered peptide solutions were incubated with solutions of $\text{Fe}(\text{NTA})$ complex at increasing concentrations. Progressive quenching of the fluorescence emission maxima was observed as iron(III) levels increased (Fig. 3b and d), suggesting that upon metal-

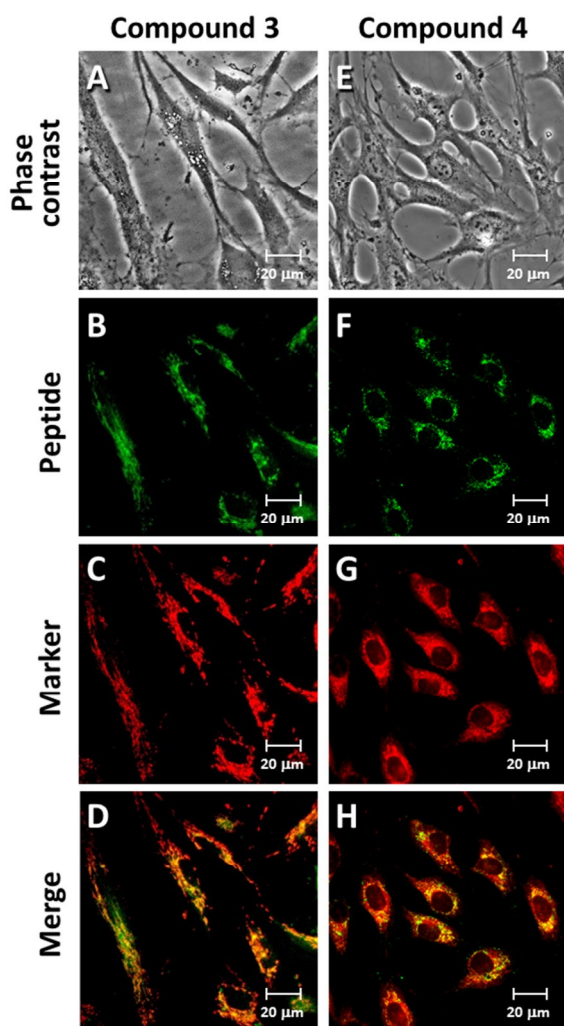


Fig. 4 Representative microscopy images of subcellular localization studies of **3** and **4** in FEK4 cells. Phase contrast images (**A**, **E**) corresponding to the fluorescence images. Following incubation with the labelled peptides (**B**, **F**), cells were treated with MitoTracker® Deep Red FM (**C**, **G**) for 30 min, rinsed and analysed by microscopy. Green and red fluorescence data were merged together (**D**, **H**) to identify co-localization in yellow. Fluorescence data were collected and analysed as described in ESI.

ligand complexation the probes were able to sense levels of iron(III) via an energy-transfer mechanism. This process was clearly dependent on iron(III) chelation since the fluorescence intensity of control peptide **8** was not influenced by the presence of iron(III) (Fig. 3c and d).

For the biological evaluation of the compounds, we first established that the compounds were effectively taken up by FEK4 cells (Fig. S7). We then carried out MTT assays and established that the compounds exhibited no cytotoxicity in FEK4 cells up to the highest tested concentration of 100 μM overnight (Fig. S6). Subcellular distribution of the fluorescent peptides in live cells co-labelled with a commercial fluorescent marker specific for mitochondria was then examined qualitatively (Fig. 4 and Fig. S4) and quantitatively (Fig. S5) using microscopy on human skin fibroblast cells in culture, as described in section Live cell microscopy of ESI. Peptides **3-4** are able to penetrate

cells (Fig. S7) and preferentially accumulate to mitochondria (Fig. 4). Similar profiles were observed for peptides **5**, **11** and **12** (Fig. S5), suggesting that the positioning of the iron chelating probe did not significantly alter the mitochondrial-targeting ability of the resultant peptides. Analysis of intensity profiles (e.g. Fig. S4b) confirmed the conclusions obtained from both qualitative and quantitative analyses of microscopy images. In contrast to the peptides investigated above, peptide **7** was found not to penetrate cells (results not shown), probably due to its lower net positive charge. The cationic amphipatic peptides such as compounds **3-5** and **11-12** are able to permeate the cell membrane and preferentially accumulate to mitochondria most likely by virtue of this organelle's high membrane potential. Such considerations denote the importance of the correct structural design of the tetrapeptide scaffold in determining its biological distribution.

To illustrate the iron responsiveness of our innovative compounds in cells, FEK4 fibroblasts were treated with compound **3** as an example and the level of intracellular iron(III) was manipulated using iron(III) (8-hydroxyquinoline)₃ ($\text{Fe}(\text{HQ})_3$) complex and the iron chelator deferiprone (DFP). The effect on the fluorescence of the labelled peptide was then registered as described previously.

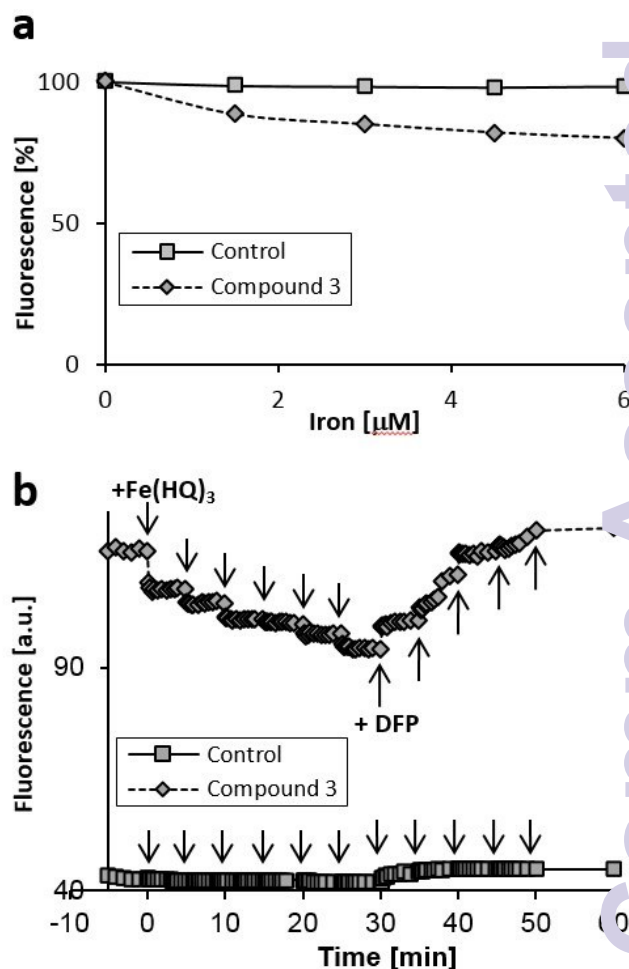


Fig. 5 Fluorescence quenching and dequenching of compound **3** in FEK4 cells in response to the manipulation of cellular levels of iron. Cells incubated (or not) with the chelator-peptide were loaded with iron(III) in the form of $\text{Fe}(\text{HQ})_3$ as described in section Fluorescence quenching/dequenching assays of ESI and then treated with the iron-specific chelator DFP. A representative

experiment is depicted. Plots of fluorescence as a function of total iron(III) concentration added (a) and as a function of time (b).

Addition of 1.5 μM increments of $\text{Fe}(\text{HQ})_3$ to compound **3**-
5 treated cells induced a progressive decrease in fluorescence when
compared to untreated control cells (Fig. 5a and b). Subsequently,
dequenching of the fluorescent signal was demonstrated upon an
initial addition of 10 μM , followed by 20 μM increments of the
10 potent iron-specific and membrane-permeable chelator
deferiprone, showing that compound **3** is not only responsive to
iron addition, but also to iron removal from cells (Fig. 5b).

The newly developed iron-binding peptides represent an
improved design to selectively deliver iron probes to
mitochondria and have the potential to measure LIP levels
15 both under physiological and various pathological conditions
involving high mitochondrial LIP levels.

Notes and references

^a Institute of Pharmaceutical Science, King's College London,
20 Franklin-Wilkins Building, 150 Stamford Street, London SE1 9NH,
United-Kingdom. E-mail: robert.hider@kcl.ac.uk; Fax: +44
(0)2078486394

^b Department of Pharmacy & Pharmacology, University of Bath,
Claverton Down, Bath BA2 7AY, United-Kingdom.

[†] Electronic supplementary information (ESI) available: Compound
25 synthesis, detailed experimental methods, HPLC chromatograms, HRES
MS data, UV-vis and fluorescence spectra of peptides, quenching assays.
Fluorescence microscopy images and intensity profiles, quantitative
analysis of co-localization, concentration curve of peptide uptake by cells.

[‡] See DOI: 10.1039/c000000x/

[§] These two authors contributed equally to this work.

1. A. H. V. Schapira, *Lancet*, 2006, **368**, 70-82.
- 35 2. A. Aroun, J. L. Zhong, R. M. Tyrrell and C. Pourzand, *Photoch
Photobio Sci*, 2012, **11**, 118-134.
3. C. C. Winterbourn, *Nat Chem Biol*, 2008, **4**, 278-286.
4. C. Pourzand, R. D. Watkin, J. E. Brown and R. M. Tyrrell, *Proc.
Natl. Acad. Sci. U. S. A.*, 1999, **96**, 6751-6756.
- 40 5. R. J. Castellani, P. I. Moreira, G. Liu, J. Dobson, G. Perry, M. A.
Smith and X. W. Zhu, *Neurochem. Res.*, 2007, **32**, 1640-1645.
6. D. J. Hare, P. Lei, S. Ayton, B. R. Roberts, R. Grimm, J. L. George,
D. P. Bishop, A. D. Beavis, S. J. Donovan, G. McColl, I. Volitakis,
C. L. Masters, P. A. Adlard, R. A. Cherny, A. I. Bush, D. I.
45 Finkelstein and P. A. Doble, *Chem Sci*, 2014, **5**, 2160-2169.
7. R. A. Vaubel and G. Isaya, *Mol Cell Neurosci*, 2013, **55**, 50-61.
8. M. P. Murphy, *Bba-Bioenergetics*, 2008, **1777**, 1028-1031.
9. K. S. Zhao, G. M. Zhao, D. L. Wu, Y. Soong, A. V. Birk, P. W.
Schiller and H. H. Szeto, *J. Biol. Chem.*, 2004, **279**, 34682-34690.
- 50 10. H. H. Szeto, *AAPS J.*, 2006, **8**, E277-E283.
11. M. P. Pereira and S. O. Kelley, *J. Am. Chem. Soc.*, 2011, **133**, 3260-
3263.
12. V. Abbate, O. Reelfs, R. C. Hider and C. Pourzand, *Biochem. J.*,
2015, **469**, 357-366.
- 55 13. Y. Ma, X. Kong, V. Abbate and R. C. Hider, *Sensor Actuat. B-
Chem.*, 2015, **213**, 12-19.

14. G. Turcatti, S. Zoffmann, J. A. Lowe, S. E. Drozda, G. Chassaing, T.
W. Schwartz and A. Chollet, *J. Biol. Chem.*, 1997, **272**, 21167-
21175.
- 60 15. Z. D. Liu and R. C. Hider, *Medicinal Research Reviews*, 2002, **22**,
26-64.